Early-Stage Reactions in Synthesis of TPA−Silicalite-1: Studies by in Situ Calorimetry, SAXS, and pH Measurements

Sanyuan Yang and Alexandra Navrotsky*

Thermochemistry Facility and NEAT ORU, University of California at Davis, Davis, California 95616

Received December 4, 2003. Revised Manuscript Received June 14, 2004

In situ calorimetry, small-angle X-ray scattering, and pH measurements were used to investigate early stages of nanopatticle formation during early stages of synthesis of silicalite-1 in an initially clear solution ($9TPAOH-25SiO_2-480H_2O-100C_2H_5OH$, TPA = tetrapropylammonium). The solution was prepared by incremental addition of tetraethyl orthosilicate (TEOS) (from 0% to 100% of the required amount) relative to a given amount of TPAOH solution. The reaction is strongly exothermic (ca. −100 kJ/mol-Si) at early TEOS additions. Part of the observed exothermic effect at this stage is attributed to the mixing enthalpy of ethanol (byproduct from hydrolysis of TEOS) with the solution and the acid−base reaction reflected by the decrease in the net hydroxide concentration in solution. With increased TEOS addition, the reaction becomes less exothermic and then the reaction enthalpy levels off at 50% addition of TEOS at −50 ± 2 kJ/mol-Si. At 50−60% addition of TEOS, the reaction rate gradually decreases to a minimum and thereafter increases. With increase of TEOS addition up to 40%, the mass of the nanoparticles formed in the solution only increases slightly and their size remains about 2.2 nm in diameter. Not until over 60% addition of TEOS is a rapid growth of their size and mass seen. The analysis and implication of the experimental results to the evolution of the nanoparticles are discussed.

Introduction

TPA−silicalite-1 with a crystal size of ca. 100 nm can be synthesized from initially clear solutions typically prepared by hydrolysis of tetraethyl orthosilicate (TEOS) in aqueous tetrapropylammonium (TPA) hydroxide solution at room temperature.[1−5] The so-called initially clear solutions are actually not true solutions because most of the silica is already polymerized to subcolloidal particles of a TPA−silica composite based on evidence from small-angle X-ray and neutron scattering (SAXS/SANS).[6,7] Ravishankar et al.[8] recently studied the nanoparticles isolated from the solution by chemical extraction and concluded that they have a well-defined TPA-MFI-crystal-like structure and composition. In a more recent study, Kragten et al.[9] presented new evidence indicating that the nanoparticles isolated from the solution by chemical extraction is essentially amorphous silica containing some bulklike TPA. It remains unclear if the isolation process by chemical extraction alters the structure of the nanoparticles.

In our previous studies using in situ calorimetry and other complementary techniques, we investigated the crystallization of TPA−silicalite-1 from initially clear solutions at 95 °C.[3,10] Our results demonstrated that crystal growth proceeds exothermally ($\Delta H < 0$) at early stages but endothermally ($\Delta H > 0$) at late stages. The exo−endo switch is associated with a change in the solution alkalinity. It is not the change in enthalpy but that in entropy ($\Delta S > 0$) that constantly drives the spontaneous crystallization forward. The entropy driving force is mainly attributed to the release into solution of water and hydroxyl molecules from the eliminated surface of the growing silicate particles. After these initial studies, we found it interesting to extend our investigation using in situ calorimetry to the early-stage zeolite synthesis events, i.e., formation of the nanoparticles from the initial reactants.

In this work we prepared a series of initially clear solutions using a fixed amount of TPAOH solution and variable amounts of TEOS. We used in situ calorimetry to measure the overall enthalpy change and monitor the evolution of the associated reactions. We used SAXS to examine the emergence and growth of the primary

(1) Nikolakis, V.; Kokkoli, E.; Tirrell, M.; Tsapatsis, M.; Vlachos, D. G. *Chem. Mater.* **2000**, *12*, 845.
(2) Ravishankar, R.; Kirschhock, C.; Schoeman, B. J.; Vanoppen, P.; Grobet, P. J.; Storck, S.; Maier, W. F.; Martens, J. A.; De Schryver, F. C.; Jacobs, P. A. *J. Phys. Chem. B* **1998**, *102*, 2633.
(3) Yang, S.; Navrotsky, A. *Chem. Mater.* **2002**, *14*, 2803.
(4) Schoeman, B. J. *Zeolites* **1997**, *18*, 97.
(5) Schoeman, B. J.; Regev, O. *Zeolites* **1996**, *17*, 447.
(6) Watson, J. N.; Iton, L. E.; Keir, R. I.; Thomas, J. C.; Dowling, T. L.; White, J. W. *J. Phys. Chem. B* **1997**, *101*, 10094.
(7) De Moor, P.-P. E. A.; Beelen, T. P. M.; Komanschek, B. U.; Beck, L. W.; Wagner, P.; Davis, M. E.; Van Santen, R. A. *Chem.-Eur. J.* **1999**, *5*, 2083.
(8) Ravishankar, R.; Kirschhock, C. E. A.; Knops-Gerrits, P.-P.; Feijen, E. J. P.; Grobet, P. J.; Vanoppen, P.; De Schryver, F. C.; Miehe, G.; Fuess, H.; Schoeman, B. J.; Jacobs, P. A.; Martens, J. A. *J. Phys. Chem. B* **1999**, *103*, 4960.
(9) Kragten, D. D.; Fedeyko, J. M.; Sawant, K. R.; Rimer, J. D.; Vlachos, D. G.; Lobo, R. F.; Tsapatsis, M. *J. Phys. Chem. B* **2003**, *107*, 10006.
(10) Yang, S.; Navrotsky, A.; Wesolowski, D. J.; Pople, J. A. *Chem. Mater.* **2004**, *16*, 210.

10.1021/cm035272q CCC: $27.50
Published on Web 08/25/2004

particles with incremental additions of TEOS. We used pH measurements to estimate the free base concentration in the initially clear solutions. Our objectives were to examine the thermochemistry of the reaction events and correlate them with the evolution of the precursor particles and the changes in solution chemistry.

Experimental Section

Preparation of Initially Clear Solutions (ICS). In this study an ICS having a composition of $9TPAOH{-}25SiO_2{-}480H_2O{-}100C_2H_5OH$, where the coefficients reflect the relative molar ratios of the components, is regarded as the standard ICS, mainly because this composition has been previously used for synthesis of TPA−silicalite-1.[3,4,10] We use ICS(*f*) to designate an ICS prepared using an "*f*" fraction ($0 \leq f \leq 1$) of the amount of tetraethyl orthosilicate (TEOS) required for the standard ICS. ICS(0) is the TPAOH solution prior to addition of any TEOS and has a composition $9TPAOH{-}430H_2O$.

TPAOH solution (Alfa, 40%), TEOS (Alfa, 99.9%), and deionized water were used as received. The preparation procedure was similar to that used in our previous reports. The TEOS phase and the aqueous TPAOH solution were initially not miscible, forming an emulsion-like mixture under stirring. After several hours of vigorous stirring at room temperature, all the mixtures became homogeneous and completely clear to the naked eye. The solutions prepared in this way were used for SAXS and pH measurements.

Calorimetric Measurement. An isothermal calorimeter (Hart, Model CSC 4400) operated under gentle stirring (60 rpm) at 25.00 °C was used. The energy equivalent of the calorimetric signal was calibrated electrically and checked by using the dissolution enthalpy of KCl. In the in situ calorimetric measurements of the ICS(*f*) formation, 25.00 g of TPAOH solution ($9TPAOH{-}430H_2O$) was contained in a Teflon cell. After stabilization (ca. 3 h), a controlled amount (ca. 200 mg) of TEOS was syringed into the cell through a Teflon-capillary-tube connection. When the reaction was over (indicated by the re-establishment of the initial flat baseline), another dose of TEOS was added. The same procedure was repeated until the total 6.866 g of TEOS was added. The final solution corresponds to ICS(1). The heat flow curve recorded for each dose of TEOS was used for the thermochemical analysis of ICS formation at the corresponding *f*.

To measure the mixing/dilution enthalpies of ICS(*f*) by water and ethanol, 25.00 g of ICS(*f*) was contained in a Teflon cell. After stabilization, 50.0 mg of water or 39.7 mg of ethanol was injected into ICS(*f*), respectively. The integrals of the heat flow peaks were taken as the corresponding dilution enthalpies at 25.00 °C.

The blank heat effects of sampling (introducing a liquid to the cell) were measured by adding a liquid at room temperature (ca. 23.5 °C) to the cell containing the same liquid at 25.00 °C. We found that these enthalpies are less than 0.1 kJ/mol for water, ethanol, and TEOS, which is comparable to the experimental errors and negligible relative to the magnitude of the reaction enthalpies. For this reason, the calorimetric data were not corrected for the blank heats of sampling.

The combined volume of the solutions is essentially unchanged by reaction and/or mixing liquids at the experimental conditions. We use the terms "enthalpy", "energy", and "energetics" essentially interchangeably because the difference between ΔE and ΔH is negligible.

Small-Angle X-ray Scattering (SAXS). The SAXS data were collected at Station BL1-4 of the Stanford Synchrotron Radiation Laboratory. A monochromatic X-ray beam (wavelength 0.1488 nm, beam size 500 μm (horizontal) and 250 μm (vertical)) and a two-dimensional detector with a 1600×1600 array of 50 μm square pixels were used. The sample-to-detector distance was 390 mm. The X-ray exposure time varied from 2 to 30 min. The solution samples were loaded in Teflon cells with Kapton film windows. The scattering intensity, $I(q)$ (where q denotes the scattering vector, $q = (4\pi/\lambda)\sin(\theta)$, where λ and 2θ are the wavelength and the scattering angle, respectively), was corrected for dark current noise in the detector, absorption from the sample, and scattering from the windows. The data with q from 0.1 to 3.4 nm^{-1} were radially averaged to minimize statistical fluctuations.

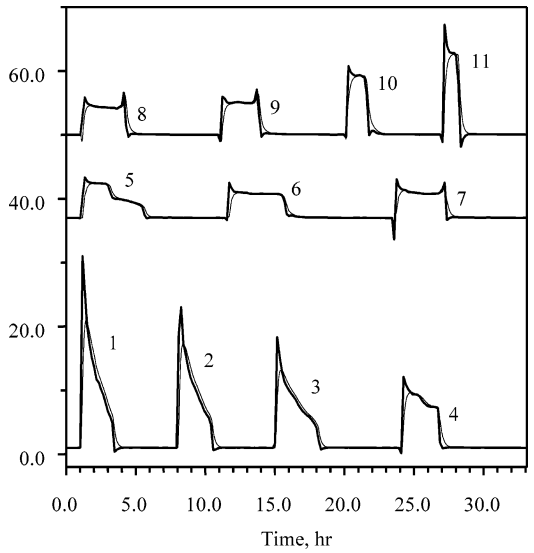

Figure 1. The directly recorded heat flow curves (thin lines) and the restored true heat flow curves (bold line) arising from reaction corresponding to incremental additions of TEOS (ca. 200 mg) to ICS(*f*) at $f = 0.065$ (1); 0.156 (2); 0.245 (3); 0.361 (4); 0.447 (5); 0.531 (6); 0.624 (7); 0.716 (8); 0.805 (9); 0.907 (10); and 1.024 (11).

pH Measurements. The pH of the aqueous solutions was measured using an Ag/AgCl Sure-Flow Electrode (Thermo Orion, Model 91-72BN). The electrode was calibrated using two standard buffer solutions (pH = 7.0 and 10.0) prior to each use.

Results

Calorimetric Measurements. Despite the convolution of the reaction heat flow curve due to the relatively slow calorimeter response, the true heat flow, $\Phi(t)$, arising from the reaction can be reconstructed from the directly measured heat flow, $\phi(t)$, by applying the following equation[11,12]

$$\Phi(t) = \phi(t) + \tau \frac{d\phi(t)}{dt} \qquad (1)$$

where τ is a time constant characterizing the calorimeter's response to a thermal perturbation. The deconvoluted heat flow curves in Figure 1 represent the thermal effect of the reaction following incremental additions of TEOS to ICS at 25 °C. The corresponding (convoluted) heat flow curves directly recorded on the calorimeter are also shown in Figure 1. A positive heat flow peak relative to the baseline means an exothermic reaction and the return of the initial baseline indicates the completion of the reaction. The variation in the peak width suggests that the overall reaction rate gradually decreases from $f = 0$ to $f = 0.5{-}0.6$. Thereafter, the rate increases with increasing *f*.

(11) Schoenitz, M.; Navrotsky, A.; Ross, N. *Phys. Chem. Miner.* **2001**, *28*, 57.
(12) Yang, S.; Navrotsky, A. *Microporous Mesoporous Mater.* **2002**, *52*, 93.

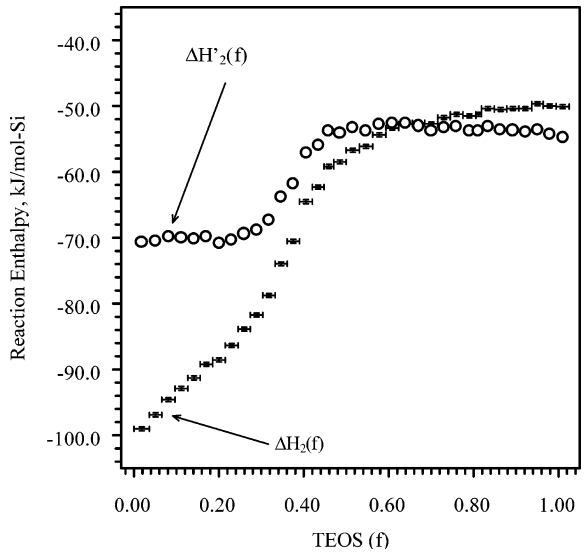

Figure 2. Reaction enthalpy, arising from incremental additions (ca. 200 mg per addition) of TEOS to 25.00 g of TPAOH solution. $\Delta H'_2(f)$ represents the reaction enthalpy after eliminating the enthalpy contributions to $\Delta H_2(f)$ due to mixing of ethanol and water with ICS(f); see text for details. Note that the error bar of f represents the range over which $\Delta H_2(f)$ is averaged; the error bar of $\Delta H_2(f)$ represents the estimated difference in repeated measurements.

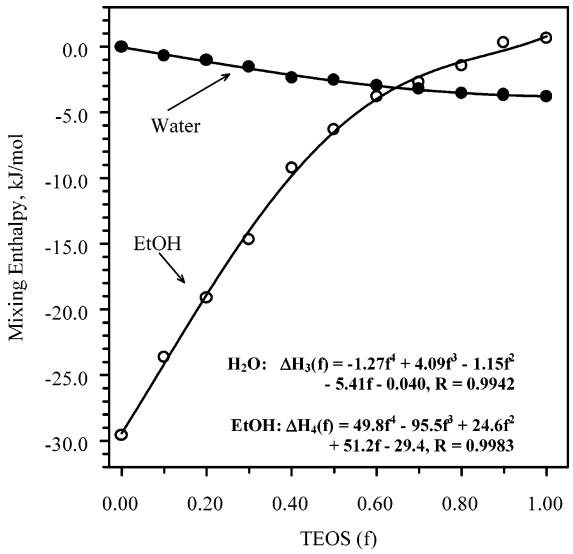

Figure 3. Polynomial fitting of the dilution enthalpy of ICS-(f) with H_2O ($\Delta H_3(f)$) and EtOH ($\Delta H_4(f)$).

Because the amount of TEOS in each addition (ca. 200 mg) is small relative to the total amount (6866 mg) of TEOS added to the 25.00 g of ICS(0), the integral of each heat flow peak was used to estimate the enthalpy, $\Delta H_2(f)$, of the following reaction,

$$\Delta H_2(f): \quad \text{TEOS(p)} \rightarrow \text{Species}(f) \tag{2}$$

where TEOS(p) indicates the TEOS in its pure liquid state and Species(f) represents the species derived from TEOS after its reaction with ICS(f). Since all the reactions are at 25 °C, for simplicity we omit the designation of temperature throughout this paper.

The evolution of ICS with incremental additions of TEOS is described by reaction 2. Note that the silicate speciation is presumably a function of f. The associated $\Delta H_2(f)$ versus f is presented in Figure 2. The overall reaction is exothermic from $f = 0$ to $f = 1.0$. The magnitude of $\Delta H_2(f)$ decreases at a nearly linear rate from $f = 0.0$ to $f = 0.2$ and then at a higher rate from $f = 0.2$ to $f = 0.5$. From $f = 0.5$ to $f = 1.0$, the heat released from the reaction gradually levels off. Because hydrolysis of TEOS consumes water and yields ethanol, the dilution enthalpies of ICS(f) with respect to water ($\Delta H_3(f)$) and ethanol ($\Delta H_4(f)$) contributes to the measured $\Delta H_2(f)$. For a complex and specific solution like ICS, to our knowledge, neither experimentally measured data nor theoretical calculations for $\Delta H_3(f)$ and $\Delta H_4(f)$ are published. We evaluate these dilution enthalpies based on direct experimental data as follows. At 11 evenly spaced f values, the enthalpies of mixing 50.0 mg of water with 25.00 g of ICS(f) were measured by calorimetry. Similarly, the enthalpies of mixing 39.7 mg of ethanol with ICS(f) were obtained. Because the amount of the added solvent is very small relative to 25.00 g of solution (roughly 1:1000 in volume/mass ratio), the measured enthalpies were used to calculate the dilution enthalpy of ICS(f) with water or ethanol. The dilution processes are written as

$$\Delta H_3(f): \quad \text{H}_2\text{O(p)} \rightarrow \text{H}_2\text{O}(f) \tag{3}$$

$$\Delta H_4(f): \quad \text{EtOH(p)} \rightarrow \text{EtOH}(f) \tag{4}$$

where p indicates the solvent molecules in their pure liquid states and f the solvent molecules in ICS(f). The plots of $\Delta H_3(f)$ and $\Delta H_4(f)$ versus f each exhibits a smooth curve. Each set of data was fitted to a polynomial equation (Figure 3). The excellent fit permits us to calculate $\Delta H_3(f)$ and $\Delta H_4(f)$ at any given f.

The reaction of each TEOS molecule in ICS consumes 2−4 water molecules and produces 4 ethanol molecules. Based on the data in Figure 3, we can subtract the enthalpy contributions of mixing ethanol and water with ICS(f) to the overall reaction enthalpy arising from incremental addition of TEOS to TPAOH solutions; see the $\Delta H'_2(f)$ curve in Figure 2. The remaining enthalpy is the quantity of interest.

SAXS Measurements. SAXS spectra of ICS(f) at various f are presented in Figure 4. All spectra exhibit a single peak with a maximum located at increasing q values with increasing f. This peak is attributed to an interference effect in X-ray scattering amplitude caused by the presence of nanometer-sized particles in the solution.[13] The average and most probable size (d) of these nanoparticles can be estimated using the equation below,

$$d = 2\pi/q_{\max} \tag{5}$$

With increasing f from 0.1 to 0.5, the size of the nanoparticles observed from SAXS increases slightly from 2.2 to 2.5 nm (Figure 5). From $f = 0.5$ to $f = 1.0$, there is a rapid increase in the size of the nanoparticles. Thereafter, the increase levels off (note that we prepared two additional synthesis mixtures at $f > 1.0$, also with appearance of a clear solution, for SAXS experiments).

(13) Glatter, O.; Kratky, O. *Small Angle Scattering;* Academic Press: London, 1982.

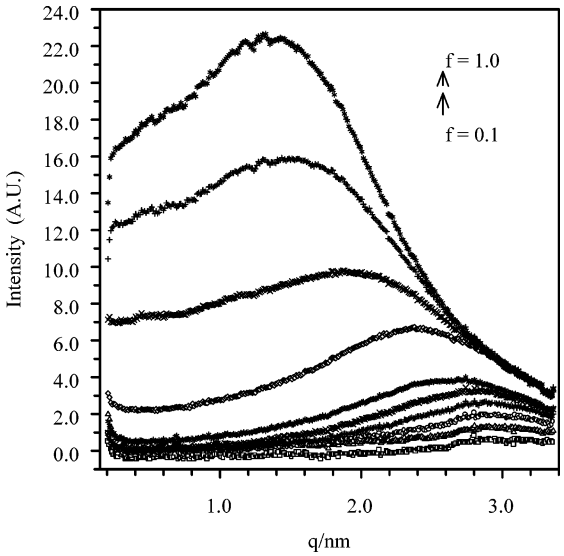

Figure 4. SAXS curve of the initially clear solution, ICS(*f*), prepared using various fractions (*f*) of the required amount of TEOS with ICS($f = 1$) corresponding to 9.00TPAOH−25.0SiO_2−480.0H_2O−100.0C_2H_5OH.

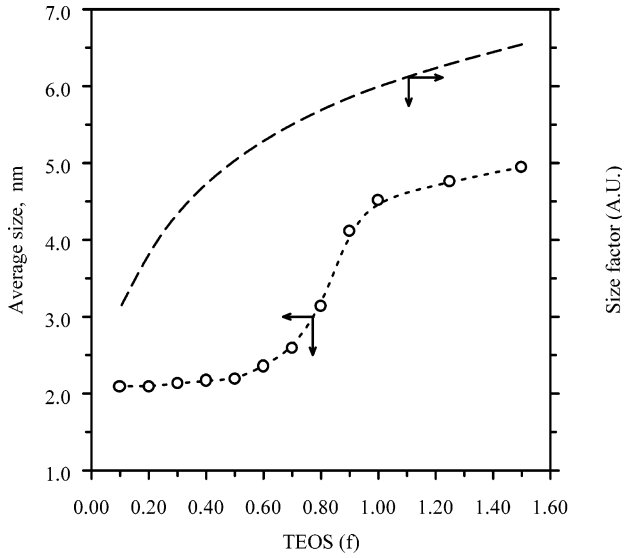

Figure 5. The average particle size by SAXS (circle) and the trend of the particle size calculated by assuming that the growth of the particle size is linearly proportional to the added TEOS and the number of particles does not increase with increasing TEOS (dashed line). Note that data with more than 100% of the required TEOS (corresponding to ICS(1)) were also included.

The stepwise growth profile of the nanoparticle size based SAXS suggests that the number of nanoparticles also increases with incremental addition of TEOS because, otherwise, a growth profile of the nanoparticles represented by the dashed line in Figure 5 would be expected. In addition, the total mass of the nanoparticles indicated by the SAXS peak height increases much more rapidly from $f = 0.6$ to $f = 1.0$ (Figure 4). These observations suggest a shift in the chemistry of ICS(*f*) near $f = 0.6$ and will be discussed below together with other experimental results.

pH Measurements. The hydroxide concentration in ICS(0) is 1.04 *m*. As TEOS is added and hydrolyzed, hydroxide will be consumed. The drop of hydroxide concentration in ICS(*f*) could be estimated by pH

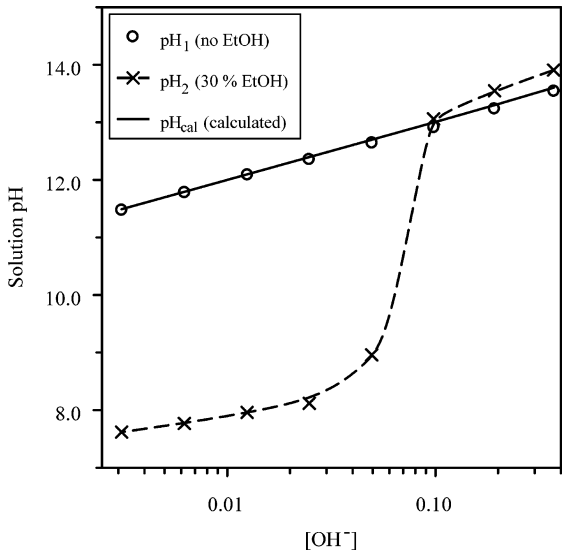

Figure 6. Comparison of the calculated pH (assuming ideal solution) and the actually measured pH of various TPAOH solutions with or without addition of 30% ethanol.

measurements. Because ICS(*f*) is a solution of very high pH (>12.5) and contains ethanol, we prepared two sets of solutions to ascertain the relation between the measured pH and the predetermined TPAOH concentration (Figure 6). Without ethanol in the aqueous TPAOH solutions, the measured pH_1 agrees excellently with $pH_{cal} = \{14 + \log(m)\}$, where *m* is the molality of TPAOH, indicating negligible ion-pair association even at pH near 14. With 30 wt % ethanol present in the solutions (note that ICS(1) contains ca. 30 wt % ethanol), at pH > ≈12.5 the measured value, pH_2, follows the same trend of pH_1 and pH_{cal} but with a small offset. At pH < ≈12.5, pH_2 differs significantly from pH_1 and pH_{cal}. It was not the intent of this study to investigate this abnormality. Since the measured pH of ICS(*f*) lies above 12.5 and ethanol content is less than 30%, for practical purposes, it is reasonable to estimate the trend of hydroxide concentration (*m*) of ICS(*f*) by

$$m_f = 10^{pH_f - 14} \tag{6}$$

The measured pH_f of ICS(*f*) at different *f* and the estimated hydroxide concentration are presented in Figure 7. The hydroxide concentration drops roughly linearly from $f = 0$ to $f = \approx 0.4$ and thereafter quickly flattens to a constant low level, ca. 0.05 *m*, at $f > 0.6$. The data in Figure 7 suggest three stages of ICS(*f*) evolution as far as variation of the hydroxide concentration and the implied net acid−base reaction are concerned: consumption of 0.8 mol of hydroxide for each mole of TEOS at $f < 0.4$ (the trend shown by the dashed line in Figure 7), a transition region at $0.4 < f < 0.6$, and no net consumption of hydroxide at $f > 0.6$.

Discussion

Hydrolysis of TEOS in aqueous solutions and the subsequent silica polymerization have been studied extensively.[14−16] The overall reaction may involve the

(14) Kirschhock, C. E. A.; Kremer, S. P. B.; Grobet, P. J.; Jacobs, P. A.; Martens, J. A. *J. Phys. Chem. B* **2002**, *106*, 4897.
(15) Sefcik, J.; McCormick, A. V. *Catal. Today* **1997**, *35*, 205.

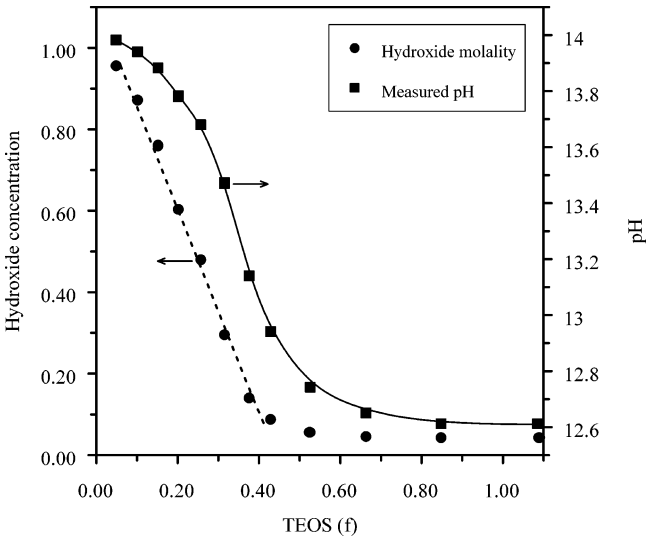

Figure 7. The measured pH of initially clear solutions and the estimated concentration of the free hydroxide.

following intertwined steps or events: (i) transfer of TEOS into aqueous solution; (ii) hydrolysis of TEOS to silicate monomer in aqueous solution; (iii) condensation/polymerization of silicate monomers to oligomers and further to precursor particles; (iv) variation of the silicate surface charge through protonation/deprotonation; and (v) intervention/interaction of TPA with hydrolyzed silicate in TEOS hydrolysis and silica polymerization. While the overall reaction can be easily tracked by in situ calorimetry, individual steps (because any one is not separated from the others in the evolution sequence) cannot be separated. Two types of data were derived from in situ calorimetric measurements. The shape of the thermal peak is related to the kinetics of the overall reaction under investigation. The integral value of the thermal peak is directly related to the enthalpy change of the overall reaction. These enthalpy values will be further analyzed below.

We stress that the integral enthalpy values are thermodynamic properties and depend only on the initial and final state of the system but not the exact path of reaction. For example, before the start of each reaction (initiated by a TEOS addition), TEOS is physically separated from the solution. At the end of reaction, the final solution is homogeneous after hydrolysis of TEOS. During part of the reaction, however, TEOS may be present as a separate phase because of the limited solubility in aqueous solution. The immiscibility decreases as more ethanol is produced (by hydrolysis). Although the rate of reaction may depend on the path (miscibility of TEOS with the aqueous solution), the overall enthalpy, being a state function, depends only on initial and final state.

Though silicate speciation in ICS(f) may be complicated at moderate silica concentration, it is presumably simple when the silica concentration in ICS(f) is infinitely low, corresponding to an ICS($f = 0$) with the extrapolated zero addition of TEOS. All the silicate species are presumably in the form of $H_2SiO_4^{2-}$ at $f \approx 0$ because of the infinitely low silica concentration (favoring the monomer) and high pH (≈14 at which $H_4SiO_4^{2-}$ is dominant).[17,18] The formation of each $H_2SiO_4^{2-}$ from TEOS, see reaction 7, consumes two hydroxides in solution.

$$\text{TEOS} + 2H_2O + 2OH^- \rightarrow H_2SiO_4^{2-} + 4\text{EtOH} \quad (7)$$

The strong exothermic effect seen by in situ calorimetry (Figure 1) is partly attributed to an acid−base reaction (see discussion below) as well as the large mixing/dilution enthalpy of ethanol with the solution (Figure 3). The data in Figure 7 show a net hydroxide consumption of ca. 0.8 OH^- per TEOS from $f = 0.03$ to $f = 0.4$. The linear drop of the net hydroxide concentration means a constant enthalpy contribution from this acid−base reaction. Since hydrolysis of each TEOS to $H_2SiO_4^{2-}$ requires two OH^-, the significantly smaller drop observed in the concentration of solution hydroxide suggests that a considerable compensation of the hydroxide concentration in solution must have occurred through polymerization of $H_2SiO_4^{2-}$, i.e., the second step of reaction 8.

$$\text{TEOS} \rightarrow H_2SiO_4^{2-} \rightarrow \text{Oligomer} \quad (8)$$

Although from $f = 0.1$ to $f = 0.4$ the total silica concentration increases by a factor of 4, the size of the nanoparticles formed in the solution remains nearly constant, ca. 2.2 nm in diameter by SAXS (Figure 5). Since the population and mass of these nanoparticles (Figure 4) remains very low, we infer that most of the silica is present as soluble species such as silicate oligomers. The detailed silicate speciation relevant to the solution system of this study is not well understood. Martens et al. used ^{29}Si NMR to investigate silicate speciation in similar clear solutions (also prepared from hydrolysis of TEOS in TPAOH solution).[14,19,20] They inferred the existence of some highly specific TPA-oligomers molecules, i.e., the subunits of the TPA-MFI structure.[14,19−21] Knight and Kinrade criticized their a priori acceptance of a molecular self-assembly theory in their interpretation of experimental data because of inconsistent observations in previous similar studies.[22] The calorimetric data of this study show an initial plateau on the $\Delta H'_2(f)$ curve ($f < 0.3$), which is consistent with the idea that TEOS is mostly converted to similar oligomers. The interpretation of the calorimetric data neither requires nor provides a detailed molecular model for such species.

In the pH range corresponding to ICS(f) from $f = 0.4$ to $f = 0.7$, $H_3SiO_4^-$ gradually becomes the dominant silicate species in a dilute solution.[14,17,18] The hydrolysis of one TEOS to $H_3SiO_4^-$ requires one hydroxide from solution (step one in reaction 9). The conversion/polymerization of a newly formed $H_3SiO_4^-$ to a Q^4-type silicate

(16) Brinker, C.; Scherer, G. *Sol−Gel Science: The Physics and Chemistry of Sol−Gel Processing*; Academic Press: London, 1990.

(17) Sefcik, J.; McCormick, A. V. *AIChE J.* **1997**, *43*, 2773.

(18) Engelhardt, G.; Michel, D. *High-Resolution Solid-State NMR of Silicates and Zeolites*; John Wiley & Sons: New York, 1987.

(19) Kirschhock, C. E. A.; Ravishankar, R.; Van Looveren, L.; Jacobs, P. A.; Martens, J. A. *J. Phys. Chem. B* **1999**, *103*, 4972.

(20) Kirschhock, C. E. A.; Ravishankar, R.; Verspeurt, F.; Grobet, P. J.; Jacobs, P. A.; Martens, J. A. *J. Phys. Chem. B* **1999**, *103*, 4965.

(21) Kirschhock, C. E. A.; Ravishankar, R.; Verspeurt, F.; Grobet, P. J.; Jacobs, P. A.; Martens, J. A. *J. Phys. Chem. B* **2002**, *106*, 3333.

(22) Knight, C. T. G.; Kinrade, S. D. *J. Phys. Chem. B* **2002**, *106*, 3329.

in the solid, donated as [SiO_2], releases one hydroxide into solution (step two of reaction 9). As a result, there is less or even no net change of hydroxide concentration in solution. Because the net hydroxide concentration in solution gradually levels off around $f = 0.4$ to $f = 0.5$, the shift of the $\Delta H'_2(f)$ curve from the initial plateau at $f < 0.3$ to a less exothermic plateau at $f > 0.5$ can be attributed to a diminishing enthalpy contribution to $\Delta H'_2(f)$ from the acid−base reaction.

$$\text{TEOS} \rightarrow H_3SiO_4^- \rightarrow [SiO_2] \qquad (9)$$

From $f = 0.4$ to $f = 0.6$, we see a gradual leveling off of the early linear drop of the hydroxide concentration in solution (Figure 7) and a slow increase in the size of the nanoparticles (Figure 5). These data imply that, for each TEOS added to the solution, the number of newly formed Q^4-type silica species gradually increases to unity at $f = 0.6$. At $f > 0.6$, no net change of the hydroxide concentration in solution and a rapid increase in the total mass and size of the nanoparticles are seen. These suggest that, for each TEOS added to the solution, the number of newly formed Q^4-type silica species is equal or even greater than unity, at the expense of the concentration of silicate oligomers in terms of silica balance (see discussion below).

With increasing TEOS addition, the pH of the ICS(f) monotonically decreases and the hydrolysis of TEOS is kinetically less favored because the reaction is base-catalyzed. With increasing TEOS addition, TEOS transfer to the aqueous solution is facilitated because of more ethanol present in the aqueous solution system. The in situ calorimetric curves (Figure 1) reveal a minimum reaction rate at $f = 0.5$ to $f = 0.6$. This minimum suggests that the polymerization−condensation of the hydrolyzed silicate species and/or TEOS transfer, rather than the hydrolysis of TEOS, controls the kinetics of the reaction. This kinetic control can be explained by considering the interplay between TEOS miscibility in the aqueous solution, solution alkalinity, and surface charge density. At $f < 0.4$, the pH is higher than ca. 13. Any pH change above 13 probably has little or no effect on the surface charge density of the silicate oligomers. This suggestion is consistent with the observation from our earlier studies that the surface charge density of silicates does not increase above a critical value during crystal growth by orderly aggregation of the precursor nanoparticles.[3,10] The linear drop of the hydroxide concentration in solution and little formation of nanoparticles at f up to 0.4 are also supportive of the presence of a saturated (or constant) surface charge density of silicate species. Since the high surface charge density prevents the silicate oligomers from polymerization/condensation to larger species, the rise in their concentration slows down the overall reaction rate with increase of f from 0.1 to 0.4. The reaction rate is lowest at $f = 0.5$ to 0.6, possibly because the concentration of the silicate oligomers reaches the highest level. With further addition of TEOS and decrease of pH to 12.6 at $f > 0.6$, the surface charge density of oligomers begins to fall below the saturation level and the aggregation of the oligomers accelerates (significant buildup of nanoparticles only at $f > 0.6$, see Figure 4). Furthermore, the slight decrease in pH and surface charge density at $f > 6$ accelerate the aggregation of oligomers to nanoparticles and/or small nanoparticles to large ones so that a decrease in the concentration of silicate oligomers is expected with increase of f.

The overlap of the $\Delta H_2(f)$ and $\Delta H'_2(f)$ curves at $f > 0.6$ (Figure 2) occurs because the enthalpy contribution from mixing ethanol or water with ICS(f) is small (Figure 3). As discussed earlier, at $f > 0.6$ the net enthalpy contributions from acid−base reactions also become negligible. Since the evolution of ICS(f) is dominated by the conversion of TEOS to silica nanoparticles, the position of the plateaus of the $\Delta H_2(f)$ and $\Delta H'_2(f)$ curves at $f > 0.6$ implies a strong energetic driving force for the evolution reaction of ICS(f), ca. −50 kJ/mol-Si. Since the size of the nanoparticles increases significantly from $f = 0.6$ to $f = 1.0$, the plateaus of the $\Delta H_2(f)$ and $\Delta H'_2(f)$ curves at $f = 0.6-1.0$ also imply a relatively small energetic difference among small and large silica nanoparticles. This absence of size dependence of energetics, though for larger zeolite nanoparticles produced in the same system, has been noted by Li et al.[23]

In conclusion, we have shown that an experimental approach based on a combination of in situ calorimetry, SAXS, and pH measurements is very powerful to investigate early events in the synthesis of TPA−silicalite-1 from initially clear solutions. In principle, the method presented in this study is applicable to the investigation of a wide variety of sol−gel processes.

Acknowledgment. This work was supported by the National Science Foundation, Grant DMR-01-01391. We also acknowledge the support of the Stanford Synchrotron Radiation Laboratory, U.S. Department of Energy, in providing the X-ray scattering facilities used in this work, supported by the Department of Energy Contract DE-AC03-76SF00515. We thank J. A. Pople (Stanford Synchrotron Radiation Laboratory) for help in SAXS experiments. We appreciate the comments by D. J. Wesolowski (Oak Ridge National Laboratory), Q. Liu (UCD), M. L. Machesky (Illinois State Water Survey), and S. I. Zones (Chevron).

CM035272Q

(23) Li, Q.; Yang, S.; Navrotsky, A. *Microporous Mesoporous Mater.* **2003**, *65*, 137.